

Atypical Transcriptional Regulation and Role of a New Toxin-Antitoxin-Like Module and Its Effect on the Lipid Composition of *Bradyrhizobium japonicum*

Paul S. Miclea,¹ Mária Péter,² Gergely Végh,³ Gyöngyi Cinege,¹ Ernő Kiss,¹ György Váró,³ Ibolya Horváth,² and Ilona Dusha¹

¹Institute of Genetics, ²Institute of Biochemistry, and ³Institute of Biophysics, Biological Research Center, Hungarian Academy of Sciences, P.O.Box 521, H-6701 Szeged, Hungary

Submitted 15 October 2009. Accepted 14 January 2010.

A toxin-antitoxin (TA)-like system (designated as *bat/bto* genes) was identified in *Bradyrhizobium japonicum*, based on sequence homology and similarities in organization and size to known TA systems. Deletion of the *bat/bto* module resulted in pleiotropic alterations in cell morphology and metabolism. The generation time of the mutant was considerably decreased in rich media. Atomic force microscopy revealed the modified shape (shorter and wider) and softness of mutant cells. The synthesis of phosphatidylcholine was completely blocked in the mutant bacteria, and vacenic acid, the predominant fatty acid of membranes of the wild-type cell, was replaced by palmitic acid in the mutant membranes. The mutant bacteria synthesized incomplete lipopolysaccharide molecules. Remarkable changes in the membrane lipid composition may explain the observed morphological alterations and growth properties of the mutant bacteria. The overlapping promoter region of *bat/bto* and *glpD* (coding for the aerobic *sn*-glycerol-3-phosphate dehydrogenase) genes suggests a complex regulation and the involvement of *bat/bto* in the control of main metabolic pathways and an important role in the maintenance of a normal physiological state of *B. japonicum*. These data reveal new aspects of the role of TA systems in bacteria.

Toxin-antitoxin (TA) modules consisting of two partially overlapping genes are ubiquitous among bacteria and archaea (Arcus et al. 2004; Gerdes et al. 2005). TA loci identified on plasmids as well as on chromosomes are characterized by similar genetic organization and regulation. Toxin genes encode proteins that recognize specific targets in the cell, and the protein products of the generally upstream-located antitoxin genes counteract the toxins by forming a complex with them. TA operons are under the negative control of the TA complex, which is able to bind to the promoter region and prevent transcription of the module (Gerdes et al. 2005).

The mechanism of action of TA systems is based on the different stabilities of toxin and antitoxin proteins; unstable antitoxins are degraded faster than stable toxins (Buts et al. 2005; Gerdes et al. 2005; Hayes 2003). The altered ratio of the two components can be induced by starvation, DNA damage, or antibiotics (Christensen et al. 2001; Hazan et al. 2004; Sat et al. 2001). The excess amount of free toxin exerts toxic effects on various cellular targets acting as DNA gyrase inhibitors,

site-specific endoribonucleases, ribosome-dependent ribonucleases, or possible ribonucleases (Arcus et al. 2004; Jensen and Gerdes 1995; Pedersen et al. 2003; Zhang et al. 2003). Plasmid-encoded systems have a clear role in plasmid maintenance by preventing the proliferation of plasmid-free progeny (Gerdes et al. 2005). The physiological function of chromosomally carried systems is still controversial, even in well-characterized cases. It has been shown that MazF of *Escherichia coli*, when activated by various stress conditions, induces significant loss of viability (Amitai et al. 2004; Hazan et al. 2004). Contrary to this observation, ectopic expression of RelE or MazF was shown to decrease cell metabolism, resulting in bacteriostasis rather than a bacteriocidal effect (Pedersen et al. 2002). The induction of the cognate antitoxins neutralized the effect of toxin molecules and cells were able to recover to normal physiology. It is possible, however, that the quasidormant state can either be reversed if stress conditions improve within a short period of time or, alternatively, after a prolonged time cells pass the ‘point of no return’ and lose the capacity to recover (Amitai et al. 2004). Recently, TA loci of chromosomal locations were also shown to participate in bacterial persistence and biofilm formation (Brooun et al. 2000; Keren et al. 2004; Lewis 2005). Since bacteria generally contain more than one TA module, the possibility that they are all involved in stress response has been investigated. Surprisingly, the absence of five copies of *E. coli* TA modules did not influence cell viability under stressful conditions (Tsilibaris et al. 2007).

The proposed role of TA loci as general stress managers adjusting metabolic rates under varying environmental stimuli may be of special importance during the adaptation of soil bacteria to oligotrophic conditions. In addition, symbiotic nitrogen-fixing soil bacteria that develop an intimate interaction with leguminous plants have the ability to adapt and function also within the plant host cells during symbiosis.

The development of symbiotic interactions of soil bacteria belonging to the genera *Rhizobium*, *Sinorhizobium*, *Azorhizobium*, *Mesorhizobium*, *Allorhizobium*, and *Bradyrhizobium* and leguminous host plants is governed by signal exchanges between the two partners. The first signals, flavonoid molecules excreted by the plants, induce the expression of bacterial nodulation genes responsible for the synthesis of bacterial signal molecules, the Nod factors (Dénarié et al. 1996). These molecules elicit the formation of new organs, the root nodules, on the plants. Nodules are invaded by symbiotic bacteria, in which *nif* genes determine the enzyme nitrogenase capable of reducing atmospheric nitrogen to ammonia (Gibson et al. 2008). The fixed nitrogen source can be utilized by the host plant; therefore,

Corresponding author: Ilona Dusha: Telephone: +36(62) 599 675; Fax: +36(62) 433 503; E-mail: dushai@brc.hu

legumes are able to tolerate nitrogen-deprived environments. The transition of free-living bacteria to the symbiotic state of bacteroids implies multiple metabolic and morphological changes, absolutely necessary for the bacteria to survive in a new environment and to perform new tasks (Jones et al. 2007).

Previously, the role of the TA locus *ntrPR* of *Sinorhizobium meliloti*, the microsymbiont of alfalfa, has been investigated (Bodogai et al. 2006). The *ntrPR* operon represents a *vapBC*-type TA system, which is the most abundant group of the seven typical TA gene families, classified according to their modular genetic organization and sequence similarities (Gerdes et al. 2005, Jørgensen et al. 2009). The antitoxin NtrP carries a SpoVT/AbrB-like domain, and the toxin NtrR contains a PIN domain (Puskás et al. 2004). The general organization and the negative autoregulation of the module are highly similar to other known TA systems. This first example of TA loci in symbiotic bacteria has been shown to have an important influence on the plant-bacterium interaction. When the toxin gene *ntrR* was inactivated by a Tn5 insertion, the mutant strain developed a higher number of root nodules on alfalfa, especially in the presence of combined nitrogen. Moreover, these bacteria induced more efficient nitrogen-fixing nodules, since bacteroids expressed *nif* genes at an elevated level (Oláh et al. 2001).

Our aim was to examine whether *vapBC*-type TA modules may also exist in the symbiotic nitrogen-fixing bacterium *Bradyrhizobium japonicum*, the microsymbiont of soybean (*Glycine max* (L.) Merr.). Soybean is an important crop used for human food and livestock feed throughout the world. Although *vapBC*-type loci represent an abundant group of TA families, their presence and copy number vary considerably in different species. *Escherichia coli*, for example, does not contain *vapBC*-type modules; in contrast, *Mycobacterium tuberculosis* and *Archeoglobus fulgidus* carry an extremely high number of PIN domain-type modules (Pandey and Gerdes 2005). By using similarity search and neighborhood analysis, we identified a putative TA-like system in *B. japonicum*. To study the role of this module, a mutant strain was constructed by deleting the whole operon. The absence of the module resulted in remarkable changes of lipid composition of membranes and caused altered generation time and cell morphology, suggesting new functions for a TA system.

RESULTS

Identification and characterization of the bsl2435/bll2434 operon, a putative TA locus in the genome of *Bradyrhizobium japonicum* USDA110.

A sequence similarity search using the deduced protein sequence of the rhizobial toxin NtrR (Oláh et al. 2001) as a query and gene neighborhood analysis pointed out a candidate TA system in the *B. japonicum* USDA110 genome. The chromosomal operon bsl2435/bll2434 (Fig. 1A), designated as a *bat/bto* operon (*Bradyrhizobium* antitoxin/*Bradyrhizobium* toxin), encodes a protein pair that forms a possible TA module. The *bat/bto* locus consists of an upstream-located 285-bp open reading frame (ORF), *bat*, that encodes a putative protein of 94 amino acids (Fig. 1B) and a downstream-located 426-bp ORF, *bto*, that encodes a putative protein of 141 amino acids (Fig. 1C). The translational start codon for *bto* overlaps with the last base of the translational stop codon of *bat*, which is a strong indication of translational coupling. The Bat protein represents the putative antitoxin component, and it carries a PhdYefM-like domain. The best-characterized member of this protein family is Phd of bacteriophage P1, the antidote partner of Doc (Lehnher et al. 1993). Smith and Magnuson (2004) proposed that TA systems are composed of two evolutionarily independent modules joined by a transition region. The first module is a

repressor represented by a DNA binding domain at the N-terminal part of the antitoxin. The second module is formed by the C-terminal part of the antitoxin and the toxin protein. Recombination in the transition region may contribute to TA diversity. Further sequence analysis revealed that the Bat protein may also be composed from two different modules. Interestingly, the N-terminal part of the protein exhibited a higher degree of identity to the Phd module (Fig. 1B), whereas the C-terminal part showed similarity to the AbrB domain of the NtrP antitoxin, a member of the *vapBC*-type *ntrPR* system of *S. meliloti* (Bodogai et al. 2006).

The Bto protein representing the putative toxin component contains a PIN domain (Fig. 1C) that has been identified in many bacteria, *Archaea* species, and eukaryota (Makarova et al. 1999). PIN domains comprise a large family of proteins characterized by the presence of four invariable acidic residues and a less conserved general amino-acid sequence identity (Arcus et al. 2004; Makarova et al. 1999). FitB, the toxin component of *fitAB* of *Neisseria gonorrhoea* (Mattison et al. 2006), presents 39% identity to the Bto protein (Fig. 1C). It is worth noting that one of the conserved aspartic acid residues at the C-terminal region is replaced by an asparagine in the Bto protein. According to these data, the structural organization of the *bat/bto* operon corresponds to that of the known bacterial TA modules.

Activity of the *bat/bto* promoter.

The negative autoregulation of TA operons by either TA complexes or free antitoxins is a common property of the characterized TA systems (Gerdes 2000; Gerdes et al. 2005; Oláh et al. 2001). To examine the regulation of the *bat/bto* operon, the plasmid pMP105, carrying the promoter region on a 379-bp fragment upstream of a promoterless *lacZ* gene, was introduced into wild-type, *bat/bto* mutant, and complemented *B. japonicum* strains, and β -galactosidase activities were determined. The enzyme activity determined in the mutant strain was considerably lower (5.2 ± 0.5 Miller units) than that in the wild-type background (114.8 ± 3.9 Miller units) (Fig. 2A, bars 2 and 1, respectively) or in the complemented strain (117.3 ± 6.1 Miller units) (Fig. 2A, bar 3), indicating that the regulation of the *bat/bto* operon does not exhibit the characteristics of typical TA modules.

Examination of the chromosomal neighborhood of the *bat/bto* operon revealed that it is located upstream of the *glpD* and downstream of the *glpR* genes (Fig 1A). The well-characterized *glpD* of *E. coli* encodes the enzyme glycerol-3-phosphate (G3P) dehydrogenase. The expression of *glpD* is negatively regulated by the repressor protein GlpR, which binds to multiple operator sequences in the *glpD* promoter (Yang and Larson 1996, 1998; Ye and Larson 1988). The presence of the inducer G3P reduces the binding activity of GlpR to the operators and thereby releases repression of the *glp* genes. The putative promoter region of the *bat/bto* operon in *B. japonicum* partially overlaps the putative promoter region of *glpD* (Fig. 2B), which is transcribed in the opposite direction from the complementary strand. Using the PromScan software, we could identify two putative GlpR binding regions in this intergenic sequence (Fig. 2B). Further examination revealed the presence of repeated sequences similar to the characteristic GlpR binding sites identified by computer-assisted analysis of *Rhizobia* (Danilova et al. 2003). The consensus sequence determined from data of three other *Rhizobium* species contains three to four direct repeats of –TTTCGTT– separated by 3 to 4 nucleotides (nt) (Danilova et al. 2003). The putative GlpR binding sites in *Bradyrhizobium* species contain two repeats without a space. One of them partially overlaps with a direct repeat sequence that, similarly to other TA modules (Bodogai et al.

2006; Magnuson and Yarmolinsky 1998; Marianovsky et al. 2001), may represent a potential binding site for the TA complex. The other putative GlpR binding site is located just upstream of the *glpD* gene. We supposed that a potential competition of the TA complex and GlpR for the overlapping binding sites in the promoter region of *bat/bto* may influence the regulation of the *bat/bto* system of *B. japonicum*.

To examine this assumption, β -galactosidase activity expressed from plasmid pMP105 was determined in wild-type bacteria grown in minimal medium (MM) containing the inducer glycerol, the precursor of G3P. The activity was considerably higher than that obtained in MM without glycerol (Fig. 2A, bars 4 and 5) demonstrating that the expression of the TA module was positively influenced, probably by the inhibition of GlpR binding. Since *bat/bto* mutant cells were not able to grow in MM, we could not perform similar experiments with strain MP99. Wild-type bacteria grown in PSY medium (peptone, salt, and yeast extract) (Hahn and Hennecke 1984) with glycerol also exhibited a higher activity level than in PSY medium without glycerol (Fig. 2A, bars 6 and 1, respectively). In contrast to other TA systems, however, the very low expression levels observed in the deletion mutant MP99, as compared with

those of the wild-type and complemented strains, indicated that the TA complex may influence its expression positively.

The effect of ectopic expression of Bat and Bto proteins on the viability of *Escherichia coli*.

To test the presumed toxic properties of the Bto protein, we examined the viability of *E. coli* strains carrying the *bto* gene and, as a control, either the *bat* gene or the *bat/bto* operon cloned in the vector pET-28. The gene expression was induced by adding isopropyl β -D-1-thiogalactopyranoside (IPTG) to the cells and, subsequently, the growth of the cultures and the number of viable cells was determined. Surprisingly, *E. coli* cells containing the *bto* toxin gene (plasmid pMP113) showed similar growth properties as the control cells carrying the vector plasmid (Fig. 3A), but the strains expressing the cloned antitoxin (pMP112) or the *bat/bto* operon (pMP114) grew very poorly (Fig. 3A). In accordance with the growth properties, the number of viable cells containing either the plasmid pET-28 or pMP113 continuously increased, whereas the living-cell number of the strains with plasmids pMP112 or pMP114 drastically decreased by the third hour after induction (Fig. 3B). These data revealed that the *bat/bto* system may be composed



Fig. 1. **A**, Organization and chromosomal neighborhood of the *bat/bto* module. The *bat/bto* operon is located between the *glpD* and *glpR* genes and is transcribed from the complementary strand in the opposite direction. The orientation and insertion site of the kanamycin-resistance cassette replacing the *bat/bto* genes in MP99 deletion mutant is shown above the module. **B**, Alignment of the deduced amino-acid sequence of the Bat protein with antitoxins Phd of phage P1 and NtrP of *Sinorhizobium meliloti*. The N terminal parts of Phd and Bat show 23% identity in 59 amino acids, but their C terminal parts are different (5.7% identity in 35 amino acids). In contrast, Bat and NtrP exhibit homology at their C terminal parts (24% identity in 34 amino acids), whereas the N terminal regions are different (16.7% identity in 60 amino acids). A recombination junction proposed for Phd antitoxin (Smith and Magnuson 2004) is also present in Bat (underlined) and is located within the transition region. **C**, Alignment of the deduced amino-acid sequence of Bto toxin with FitB, the toxin component of the *fitAB* module of *Neisseria gonorrhoea* (Mattison et al. 2006). The two sequences are 39% identical. The conserved acidic residues are shaded. The aspartate residue near to the C terminal end in FitB is replaced by an asparagine in the Bto protein.

of an active antitoxin and a functionally inactive toxin component. The more pronounced decrease of the number of viable cells in the presence of both components suggests a role for the toxin via complex formation with its antitoxin partner.

The altered division rate of the *bat/bto* mutant strain is dependent on the nitrogen and carbon sources of the growth medium.

Deletion of the *bat/bto* operon of *B. japonicum* resulted in a considerably decreased generation time of the mutant strain MP99 (2.5 h) compared with that of the wild-type bacteria (14 h) in yeast extract mannitol (YEM) medium (Fig. 4A). Growth stopped when the optical density at 600 nm (OD_{600}) of the MP99 culture reached 0.8. Under these conditions, more than 80% of the cells sustained their viability for more than 6 days. The growth of bacteria could be restored by transferring the cells into fresh medium, in which higher optical densities ($OD_{600} = 1.2$) were obtained (data not shown). In PSY medium, the generation time of MP99 was even shorter (about 2 h) and the culture could reach a much higher OD (Fig. 4B). To determine which component of the PSY medium was responsible for the improved generation time, the effect of two components, peptone and biotin, was tested by adding them separately to YEM medium. The presence of biotin did not improve bacterial growth in YEM. Moreover, biotin was also not required for the growth of wild-type *B. japonicum* strains in PSY medium (data not shown). The addition of peptone, a rich source of complex nitrogen and carbon, however, promoted a better growth of MP99 in YEM medium (data not shown), suggesting a role of the complex nitrogen source in the fast growth. This was confirmed when MM containing ammonium sulphate as nitrogen source was used. The *bat/bto* mutant was unable to grow in MM, whereas the growth of the wild-type bacteria was only delayed (Fig. 4C). When peptone was added to MM, the growth of MP99 was similar to that in YEM (Fig. 4D).

To examine whether the altered division rate of the mutant strain was due to the deletion of the *bat/bto* module, MP99 was complemented in trans with a plasmid containing the *bat/*

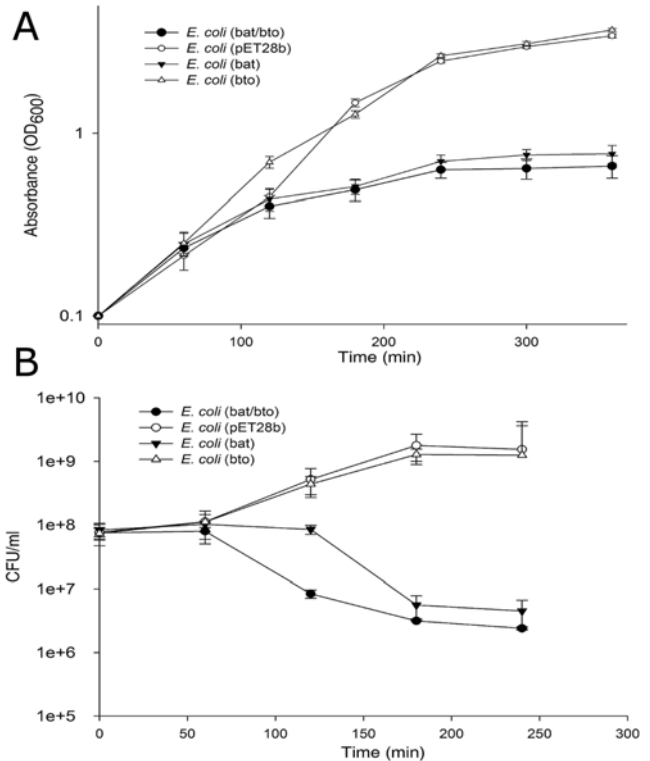


Fig. 3. A, Growth and **B**, viability of *Escherichia coli* carrying the vector plasmid (pET-28b, open circles), the cloned *bat* antitoxin (pMP112, filled triangles), the *bto* toxin (pMP113, open triangles), or both genes (pMP114, filled circles) expressed from the isopropyl β -D-1-thiogalactopyranoside (IPTG)-inducible promoter of plasmid pET-28b. *E. coli* cells grown in Luria Bertani (LB) medium were induced by 1 mM IPTG at an optical density at 600 nm (OD_{600}) = 0.1. Growth of bacteria was followed by measuring OD_{600} . Samples were taken at the indicated time and were diluted and plated on LB medium to determine the number of viable cells. Standard deviations were calculated from the results of three experiments.

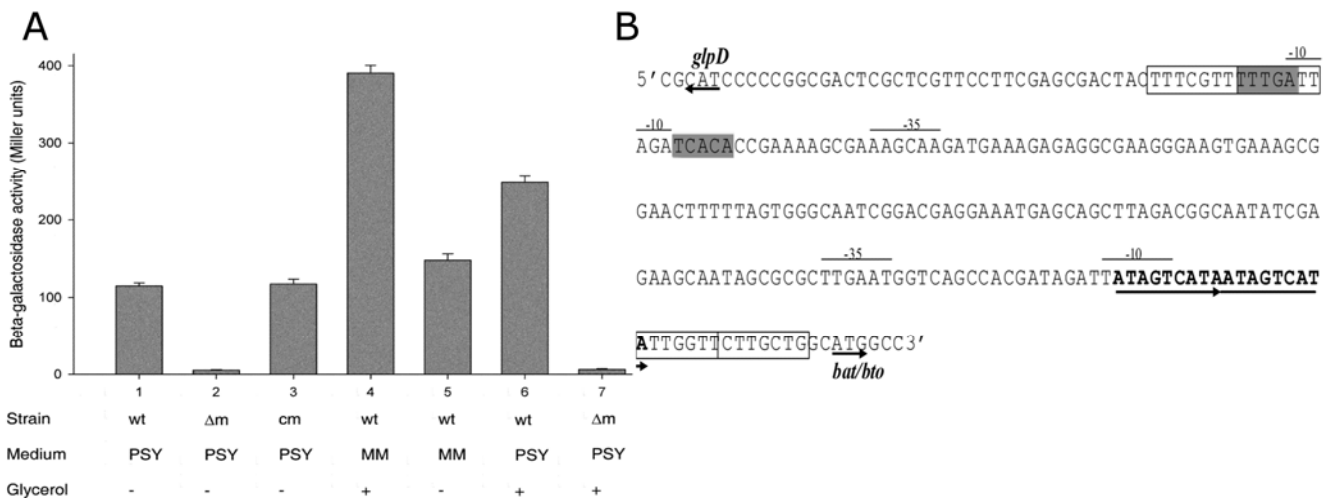


Fig. 2. A, Activity of the *bat/bto* promoter. β -galactosidase activity expressed from plasmid pMP105 carrying a 379-bp fragment consisting of the 233-bp intergenic region, 144 and 2 bp of the *glpD* and *bat/bto* coding regions, respectively. Enzyme activities of *Bradyrhizobium japonicum* wild-type (1, 4, 5, 6), MP99 deletion mutant (2, 7), and MP120 complemented (3) strains carrying pMP105 were determined. Bacteria were grown in peptone, salt, and yeast extract (PSY; 1, 2, 3, 6, 7) or in minimal medium (MM; 4, 5) at 31°C, to an optical density at 600 nm = 0.5. Cultures were induced by the addition of 0.04% glycerol as indicated. The measurements were repeated five times. Wt = wild-type strain, Δm = deletion mutant MP99, and cm = complemented strain MP120. **B**, The intergenic region of *glpD* and the *bat/bto* module with repeated sequences (ATAGTCAT) representing potential binding sites of the Bat/Bto complex (underlined with arrows). Potential -10 and -35 regions in the promoter of *glpD* and *bat/bto* are superlined. A TGN extension of the -10 motif in the *glpD* promoter region may account for the lower conservation of the -35 region. A possible CRP binding site, TTTGA-N₅-TCACA, upstream of *glpD* is shaded. Translation start sites for *glpD* and *bat/bto* are shown by small arrows. Putative GlpR binding sites exhibiting similarity to the sequence unit -TTTCGTT- characteristic for α -proteobacteria (Danilova et al. 2003) are boxed.

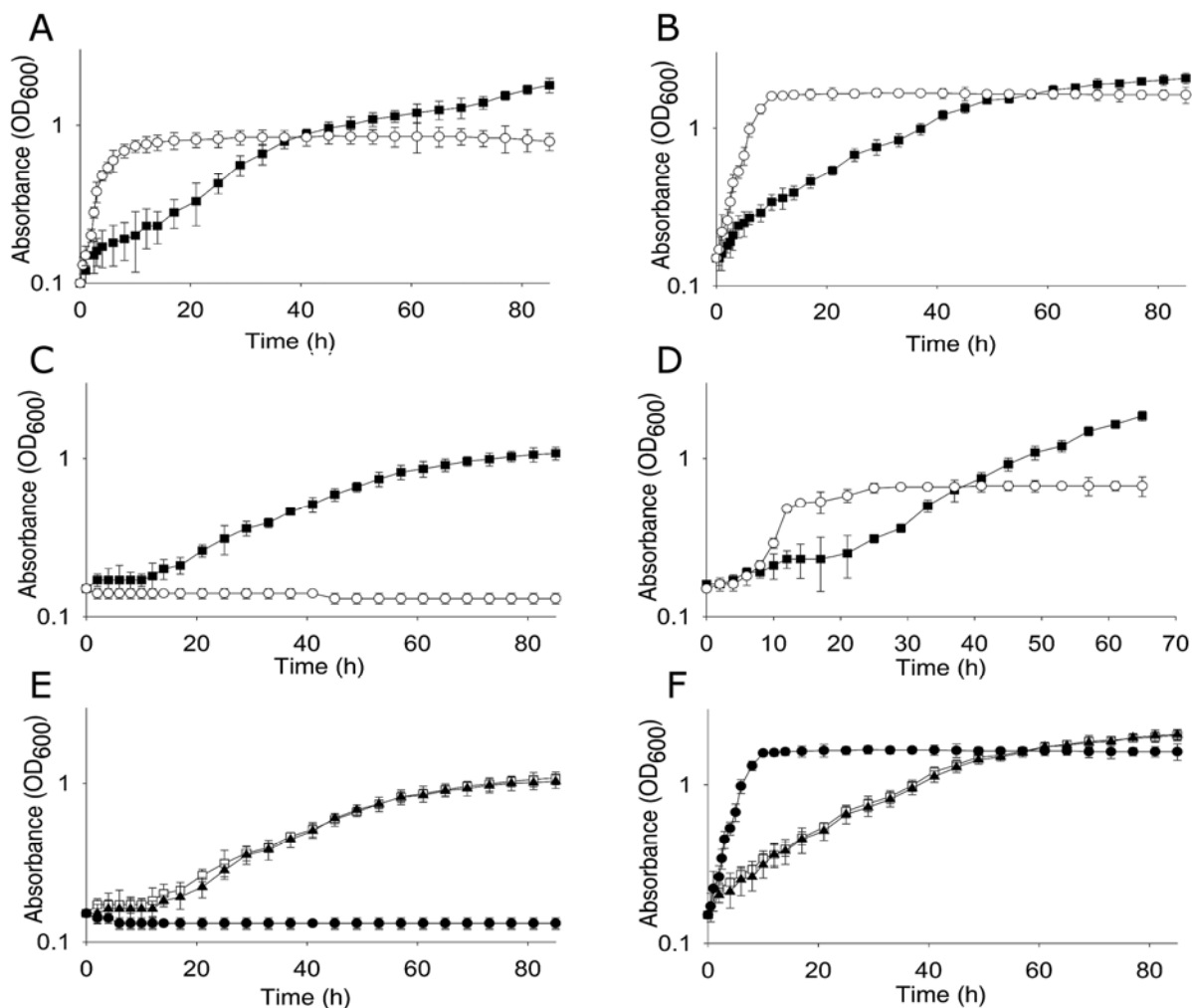


Fig. 4. A, B, C, and D, Growth curves of *Bradyrhizobium japonicum* wild-type (filled squares) and *bat/bto* mutant MP99 (open circles) strains in A, yeast extract mannitol (YEM), B, peptone, salt, and yeast extract and C, minimal medium (MM) without and D, with the addition of peptone. E and F, Comparison of the growth of *B. japonicum* wild type, deletion mutant MP99, and MP120 complemented strains in MM (E) and YEM (F) media. *B. japonicum* wild-type strain with plasmid pRK290, open squares; mutant MP99 strain with pRK290, filled circles; and complemented strain with the recombinant plasmid pMP117, filled triangles. Cultures were grown at 31°C in liquid medium containing the appropriate antibiotics. At the beginning of the experiments, starter cultures were diluted in the corresponding media to obtain an optical density of 0.15. The growth of bacteria was followed by measuring the optical density at 600 nm. Standard deviations were calculated from the data of four experiments.

bto coding region and the putative promoter. Whereas the presence of the vector plasmid pRK290 had no influence on the growth properties of either the wild-type strain or the mutant MP99 (Fig. 4E and F), the growth of the complemented strain MP120 was similar to that of the wild-type strain, both in MM and YEM media (Fig. 4E and F, respectively), suggesting that the altered generation rate of the MP99 mutant strain was due to the absence of the *bat/bto* operon. The revertant MP119 strain (obtained by restoring the *bat/bto* operon in the mutant MP99 strain) exhibited a similar growth pattern as wild-type and MP120 complemented strains (data not shown).

Cell size and mechanical parameters are affected by the *bat/bto* mutation.

The faster-dividing MP99 cells also exhibited considerably altered morphological properties (Fig. 5A). Three-dimensional surface profiles of living cells obtained by atomic force microscopy (AFM) demonstrated that wild-type bacteria had elongated cylindrical shape (2 to 2.5 μm long and 0.5 to 0.6 μm wide), whereas the mutant cells were more compact and round shaped with decreased length (1 to 1.5 μm) and increased width (1 to 1.4 μm). The height profile shown in Figure 5B was determined between the markers indicated in Figure 5A. The three-

dimensional surface profile of complemented strain MP120 showed similar elongated cylindrical cells with the same dimensions as was observed for the wild-type cells (data not shown), demonstrating that the wild-type morphology was restored by introducing the *bat/bto* genes.

Since the cell sizes of the wild-type and the mutant bacteria were remarkably different, we compared the number of colony-forming units of the two strains (grown in PSY medium) at increasing OD₆₀₀ values. The cell numbers of the wild-type strain were lower between OD₆₀₀ = 0.3 to 0.5, but the difference was not statistically significant (data not shown). At higher OD values, the cell numbers were nearly identical.

To investigate the mechanical properties of the mutant cells, local force measurements were performed by recording the indentation of the AFM cantilever in function of the vertical displacement of the z piezo. As the distance and indentation curves demonstrated, greater distance (Fig. 6A) and indentation (Fig. 6B) values were obtained with the mutant cells compared with those obtained with the wild-type strain, indicating a softer cell surface (Bálint et al. 2007). This was confirmed by the calculated elastic modulus, which was about one order of magnitude lower for the mutant strain. $E_m = 0.6 \pm 0.24$ MPa and $E_m = 4.5 \pm 0.92$ MPa for the mutant and the wild-type

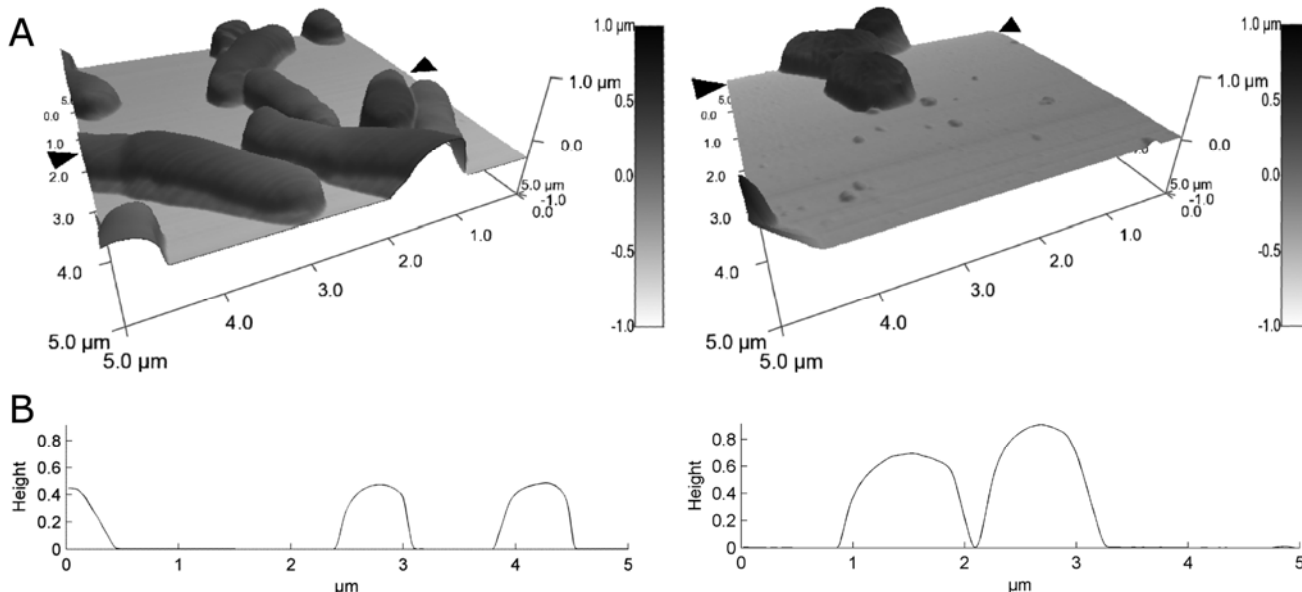


Fig. 5. A, Three-dimensional atomic force microscopy (AFM) profiles of *Bradyrhizobium japonicum* wild-type (left) and *bat/bto* mutant MP99 (right) cells constructed from 5×5 - μm scan images. Both trace and retrace images were measured at a scan rate of 0.3 to 1.0 lines s^{-1} . **B**, Height profiles of AFM images were drawn between the markers (black triangles). Images were made after immobilization of bacterial suspensions grown at 31°C in yeast extract mannitol medium on a poly-L-lysine precoated mica surface.

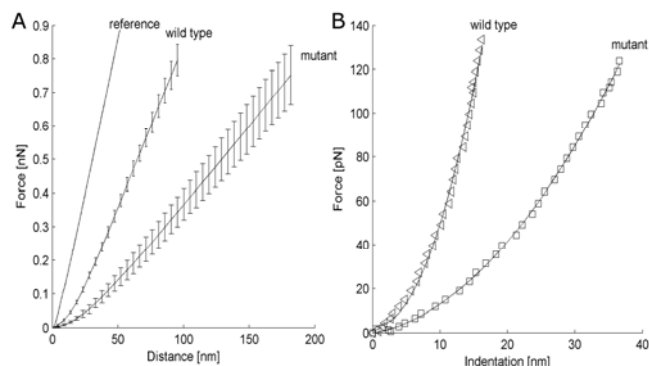


Fig. 6. Elastic properties of *Bradyrhizobium japonicum* wild-type and *bat/bto* mutant bacteria measured by atomic force microscopy. **A**, Force-distance curves with standard deviation error bars. **B**, Force-indentation curves calculated by subtracting the reference from the curves of wild-type and mutant cells. Lines are the fitted second order polynomials. Bacterial suspensions were immobilized after being grown at 31°C in yeast extract mannitol medium on a poly-L-lysine precoated mica surface.

cells, respectively. To explain the observed morphological changes, the amount and composition of several cell-membrane components of the mutant and wild-type strains were investigated in further experiments.

The *bat/bto* mutation results in differences in the pattern of lipopolysaccharides (LPS) and phospholipids (PL).

LPS contributing to the structural and physiological integrity of the bacterial cell were analyzed in further experiments. Rhizobial LPS also play an important role in the symbiotic infection process. Rhizobium mutants producing defective LPS that lack the *O*-chain polysaccharide were shown to be defective in nodulation (Stacey 1991). The differences in LPS pattern between the wild-type and MP99 strains were remarkable (Fig. 7). The heterogeneous banding region of wild-type LPS (Fig. 7, lane 1) consisted of LPS molecules that were separated according to the number of *O*-antigen repeating units or differences in the electric charges of these units (Carrion et al. 1990). The low molecular weight bands (Fig. 7, lanes 2 and 4)

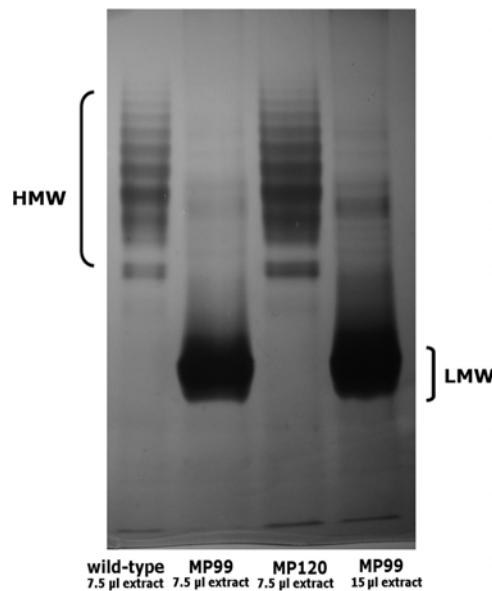


Fig. 7. Sodium deoxycholate-polyacrylamide gel electrophoresis (DOC-PAGE) of polysaccharide extracts from *Bradyrhizobium japonicum* wild-type, mutant MP99, and complemented MP120 strains silver-stained for lipopolysaccharides (LPS). Two types of LPS of differing molecular weight are indicated (HMW and LMW). Polysaccharides were extracted from cultures grown in peptone, salt, and yeast extract medium at 31°C to an optical density at 600 nm = 0.6. DOC-PAGE was performed on 18% polyacrylamide gels.

represented incomplete LPS of the mutant strain, which either lacked the entire *O*-antigen repeating unit or contained only one to two repeating units. The mutant also produced lower amounts of complete LPS molecules with altered mobility as compared with the wild-type strain (Fig. 7, lane 4). In the complemented strain MP120 that carried the reintroduced *bat/bto* operon, the heterogenous banding region characteristic for the wild-type LPS pattern was restored (Fig. 7, lane 3).

The considerable change in the shape of the cells and the softness of the mutant membrane observed by AFM force measurements suggested an alteration of the membrane com-

position of the *bat/bto* mutant. To determine the PL composition of membranes of wild-type and MP99 strains, thin-layer chromatography coupled with gas chromatographic-mass spectrometry (GC-MS) determination of fatty acids was used (Fig. 8). The main PL of the wild-type cells were phosphatidylethanolamine (PE), phosphatidylcholine (PC), cardiolipin (CL), phosphatidylglycerol (PG), the intermediate lipid mono-methyl-phosphatidylethanolamine (MMPE), and lysophosphatidylethanolamine. There were striking differences in the PL composition of the two strains (Fig. 8A and B), of which the most remarkable was the complete lack of PC in the mutant. The main PL in both cell types was PE, which increased in parallel with the disappearance of PC. CL was present in higher amounts in the mutant, at the expense of its precursor, PG.

As the physico-chemical properties of PL are determined by both the head group and the alkyl chain regions, the fatty-acid composition of total PL was also investigated from both wild-type and MP99 strains (Fig. 8C and D). In the wild-type bacteria, *cis*-vaccenic acid (18:1) was the major fatty acid, making up about 80% of total fatty acids, the amount of which decreased to less than one third (25%) in the mutant

strain. As the amount of palmitoleic acid (16:1) increased more than 50 times (0.4% in the wild-type vs. 25.2% in the mutant cells), it was obvious that fatty-acid elongation was blocked in the mutant strain. However, there was a more overall modification in fatty-acid synthesis as palmitic acid (16:0) content increased from 14% in the wild type to 42% in the mutant cells, resulting in a considerable decrease in the ratio of unsaturated fatty acids in the mutant (50.9%) compared with a much higher value in wild-type cells (83.3%), suggesting a fundamental alteration in the lipid chain order and the polymorphic characteristics of membrane lipids.

To explain the profound changes observed in PL composition, the expression of several genes involved in PC biosynthesis was investigated.

In the *bat/bto* mutant cells, transcripts for the two PL *N*-methyltransferases *PmtA* and *PmtX1* are not detectable.

Biosynthesis of PC from PE is accomplished by three successive methylation steps in many prokaryotes. An alternative direct pathway that requires the presence of free choline and of

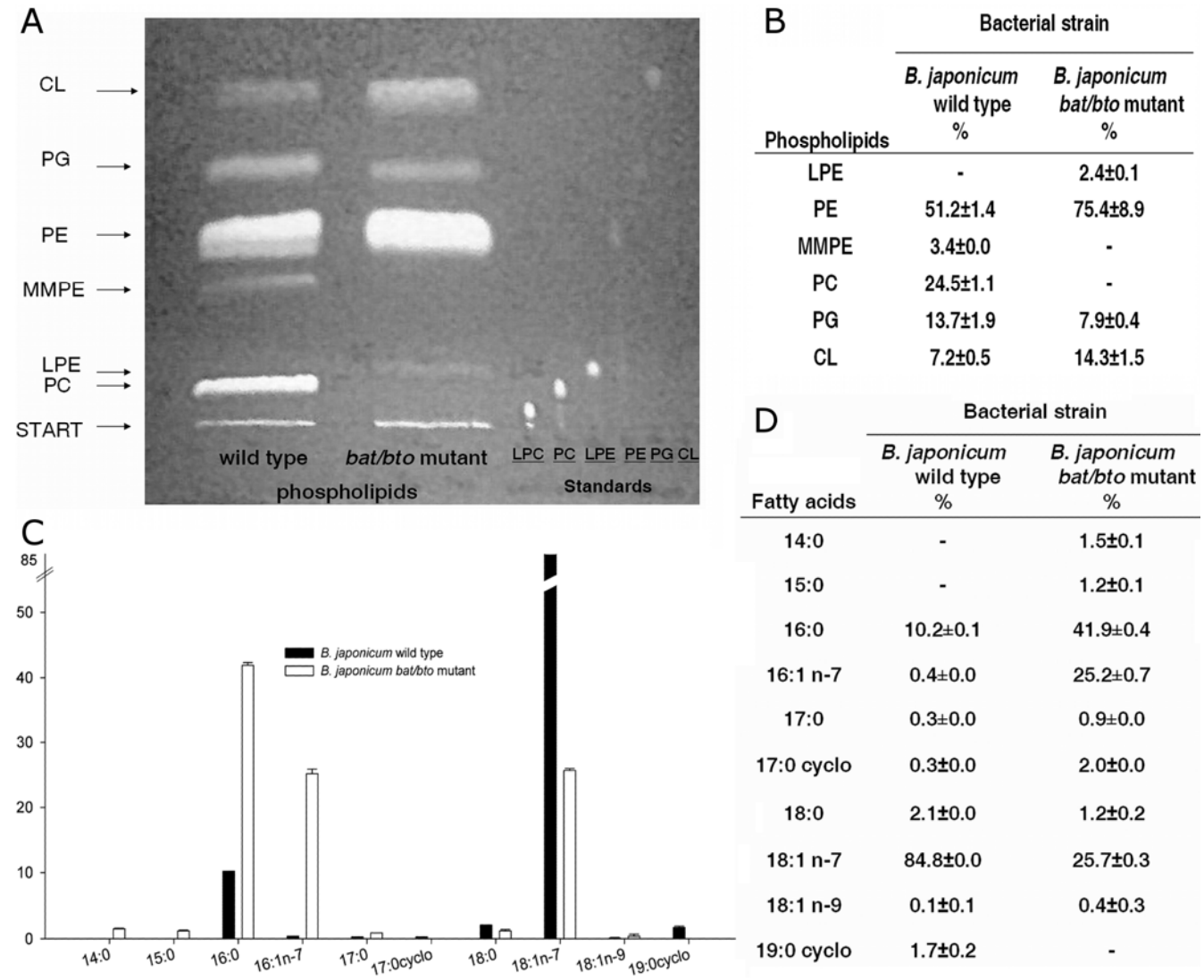


Fig. 8. Lipid analysis of *Bradyrhizobium japonicum* wild-type and MP99 mutant cells. **A**, Thin-layer chromatography of phospholipid samples performed on silica gel G plates. Samples were visualized by spraying with 0.05% 8-anilinonaphtalene-1-sulfonate. **B**, Phospholipid composition was determined after transmethylation. The identified phospholipids are: LPE = lysophosphatidylethanolamine, PE = phosphatidylethanolamine, PG = phosphatidylglycerol, CL = cardiolipin, PC = phosphatidylcholine, and MMPE = mono-methyl-phosphatidylethanolamine. **C** and **D**, Fatty-acid composition of total lipid extracts. The amount of fatty acids as the percentage of total lipids is indicated with standard deviation values. All experiments were done in triplicate.

PC synthase was documented in several bacteria (Martínez-Morales et al. 2003). The absence of PC from the membranes of MP99 mutant cells was an intriguing observation. Moreover, MMPE, the first intermediate during the conversion of PE to PC was also absent from the mutant membranes. In *B. japonicum*, the first methylation step is performed predominantly by the enzyme PmtA, whereas PmtX1 catalyzes mainly the second and third subsequent methylation steps (Hacker et al. 2008). With the use of reverse transcription-polymerase chain reaction (RT-PCR), we checked the level of mRNA from these two genes. We observed that both the *pmtA* and *pmtX1* transcripts were detectable in the wild-type cells (Fig. 9, lanes 5 and 8), but they were not detected in the mutant strain (Fig. 9, lanes 6 and 9) or in the mutant strain carrying the vector plasmid pRK290 (data not shown). In the complemented MP120 strain, *pmtA* and *pmtX1* mRNA levels were restored (Fig. 9, lanes 7 and 10). Therefore, the lack of the enzymes catalyzing the methylation reactions explained the absence of PC in the *bat/bto* mutant bacteria. As a positive control, the expression of histidyl-tRNA synthetase was detected in all strains (Fig. 9, lanes 2, 3, and 4).

Symbiotic phenotype of the *bat/bto* mutant.

We have shown previously that a mutation in the toxin component of the *ntrPR* module of *S. meliloti* results in increased nodulation and more efficient nitrogen-fixation capacity in symbiosis with the host plant alfalfa (Oláh et al. 2001). Since both toxins Bto and NtrR are PIN domain homologs, we examined whether the Bto toxin may have a similar effect on symbiotic properties. Soybean plants were inoculated with mutant MP99 and the wild-type strain, and nodule formation and plant biomass production were determined after 60 days. Deletion of the *bat/bto* region resulted in decreased symbiotic capacity. The mutant strain produced about 60% fewer nodules on soybean (51.7 ± 6 nodules per plant formed by the wild-type bacteria compared with 22.5 ± 4 nodules per plant elicited by the mutant MP99 strain). The average dry weight of plants inoculated by the mutant strain was about 40% lower than that of the wild type–inoculated plants (0.57 ± 0.13 and 0.95 ± 0.12 g per plant, respectively). The average dry weight of uninoculated plants was 0.38 ± 0.07 g per plant.

Bacteria were recovered from 40 randomly collected nodules of both types, and 200 colonies from each inoculation were tested for kanamycin and spectinomycin resistance, the markers of the mutant and wild-type strains, respectively. All of the colonies (100%) obtained from the MP99 mutant–elicited nodules were kanamycin resistant and exhibited the morphology of the MP99 mutant colonies (low levels of polysaccharide production). Their growth on YEM agar plates was also similar to that of the MP99 strain. Randomly selected colonies were further tested in YEM liquid medium, and their generation times were identical to that of the mutant strain (data not shown). The nodules elicited by the wild-type strain contained only kanamycin-sensitive bacteria.

DISCUSSION

In this paper, we report the identification and experimental characterization of the first TA-like module of the soybean microsymbiont *Bradyrhizobium japonicum*. We demonstrate that the deletion of the TA module caused remarkable physiological alterations resulting in morphological and structural changes. The observed effects define new functions for a TA system.

TA loci have been grouped into seven families based on their module organization and domain structure (Gerdes et al. 2005; Jørgensen et al. 2009). Members of the *vapBC* family are composed of a toxin carrying a PIN domain and an anti-

toxin containing one of the DNA-binding motifs AbrB, cHTH, Phd/YefM, or MetJ/CopG. The chromosomally located *bat/bto* system is composed of a Phd/AbrB-type antitoxin and a PIN domain-type toxin.

Although the size and organization of the genes and the deduced amino-acid sequences of the proteins encoded by the *bat/bto* module classified it as a TA system belonging to the *vapBC*-family, the expression of the module did not exhibit the typical negative autoregulatory properties of most TA modules. The expression level was higher in the wild-type background than in the mutant strain, suggesting a positive role for the TA complex. Since the putative binding site for the Bat/Bto complex follows the -10 region, a direct autoactivation seems unlikely. Further experiments are required to clarify this mechanism. Two modules with similar properties were identified in *Mycobacterium tuberculosis*, where RelB and RelF antitoxins acted as transcriptional activators on their respective promoters (Korch et al. 2009). However, together with their toxin pairs, these proteins repressed the expression to basal levels. The absence of a typical autorepression was also demonstrated in *Staphylococcus aureus*. The promoter of the *mazEF* module in this bacterium was downregulated by *sigB* encoding an alternative sigma factor and was activated by a SarA transcriptional regulator (Donegan and Cheung 2009). In addition to the lack of negative autoregulation of *bat/bto*, the partial overlapping of the potential binding sites of GlpR protein and the Bat/Bto complex suggested the involvement of the downstream-located GlpR protein in *bat/bto* regulation. Indeed, in the presence of the inducer glycerol, an increased promoter activity was observed in the wild-type cells grown either in rich medium or MM.

In the genome of three *Bradyrhizobium* strains (*B. japonicum* USDA 110 and *Bradyrhizobium* sp. strains BTAi1 and ORS278) one of the multiple *glpD* copies is located downstream of *glpR*. Putative GlpR binding sites could be localized only in the promoter region of these copies. However, none of these sequences contain three to four direct repeats of the consensus $-TTTCGTT-$ separated by 3 to 4 nt, as was described for three other *Rhizobium* species (Danilova et al. 2003). The *Bradyrhizobium* promoters are characterized by the presence of T-rich sequences interrupted by 2 to 3 G/C nt.

Our observation that the ectopic expression of Bto toxin had no influence on the viability of *E. coli* suggested that the Bto protein has lost its function characteristic for the toxin components of TA modules. It is conceivable that the loss of toxicity is due to the replacement of one of the essential acidic residues with an asparagine near to the C-terminal end. The structural analysis of PIN-domain proteins revealed that the quartet of acidic amino acids constitute the active site, which binds Mg^{2+} or Mn^{2+} ions and facilitates the cleavage of single-stranded

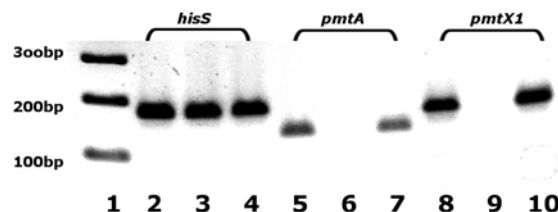


Fig. 9. Transcript levels of *pmtA*, *pmtX1*, and *hisS* genes. RNA was isolated from cultures of *Bradyrhizobium japonicum* strains grown in peptone, salt, and yeast extract medium at 31°C. Reverse transcription was performed from identical amounts of RNA obtained from *B. japonicum* wild-type (lanes 2, 5, and 8), MP99 *bat/bto* mutant (lanes 3, 6, and 9), and MP120 complemented (lanes 4, 7, and 10) strains. Amplification reactions were done using gene-specific primers for *hisS* (lanes 2, 3, and 4), *pmtA* (lanes 5, 6 and 7), and *pmtX1* (lanes 8, 9, and 10). Lane 1, DNA ladder.

RNA (Bunker et al 2008). More surprisingly, the ectopic expression of either the Bat antitoxin or the complete module resulted in a remarkable loss of cell viability. Whether these unconventional properties of the *bat/bto* system are due to the binding of antitoxin to some yet unknown regulatory regions or to possible interactions with TA modules of *E. coli* remain to be further examined.

By analyzing nearly 400 natural isolates of *E. coli*, Mine and coworkers (2009) proved that 29% of the *ccd*₀₁₅₇ variants were composed of an active antitoxin and an inactive toxin. Moreover, the CcdB toxin proteins were more diversified and lost their function more frequently than the antitoxins. Comparing the intergenic regions between *glpD* and *glpR* genes of three *Bradyrhizobium* species (*B. japonicum* USDA110 and *Bradyrhizobium* sp. strains BTAi1 and ORS278), we observed a considerable DNA sequence similarity, similar length, and the presence of identical putative binding sites for GlpR. We suppose that the *bat/bto* operon was acquired by horizontal gene transfer and was inserted between the *glpD* and the *glpR* genes of *B. japonicum* USDA110. The possible lack of stronger selective pressure may have resulted in the inactivation of toxin protein, whereas the antitoxin (and its complex with the cognate toxin) became part of a metabolic process such as the competition with the GlpR protein.

Deletion of the *bat/bto* operon resulted in alterations in several metabolic pathways leading to characteristic phenotypic changes. The electrophoretic pattern of LPS of cell membranes revealed the accumulation of incomplete LPS molecules. Comparison of the composition of PL and fatty acids in the wild-type and mutant strains showed substantial alterations. PC was completely absent in the mutant strain, whereas PE together with CL increased dramatically. It is known that PE and CL are both non-bilayer forming lipids. In the cells, the balance between bilayer and nonbilayer lipids is tightly regulated and has been shown to be essential for viability (Rietveld et al. 1993). The regulation of the tendency to form the hexagonal phase can be achieved by alterations in membrane fatty-acid composition that influence PL shape (Horváth et al. 1986). The cone-shaped geometry of PE with relatively small head group size coupled with the relatively large area occupied by the unsaturated 18:1 acyl chains promotes the formation of nonbilayer, hexagonal structures. This might explain why the content of unsaturated fatty-acid species (18:1) decreased in the mutant strain, which had a dramatically increased PE content. Taken together, it is highly conceivable that the above restructuring of lipids is aimed at reestablishing lateral packing order, bilayer stability, membrane permeability, and ultimately, membrane functionality in the mutant strain (Vigh et al. 2005).

In prokaryotes, one of the biosynthetic pathways to yield PC is the enzymatic methylation of PE catalyzed by PL *N*-methyltransferase (Pmt) in three consecutive steps using *S*-adenosylmethionine as methyl donor. Alternatively, PC can be synthesized directly from free choline by PC synthase (Pcs). Pcs is also present and functional in *B. japonicum*, although no uptake system exists for choline in this species (Boncompagni et al. 1999; Hacker et al. 2008). The block of the methylation pathway results in the complete absence of PC in the MP99 mutant strain. We have shown that the methylation steps are defective, since the transcripts of the genes coding for PmtA and PmtX1 (Hacker et al. 2008) were not detected in the mutant cells. We suppose that the absence of Bat/Bto indirectly affects these transcript levels either via the activation of a degrading factor or by influencing an unknown positive regulatory factor involved in the transcription of these genes.

The profound alterations in the lipid composition of the mutant membranes may result in changes in the cell division rate, cell shape, and membrane rigidity. Distribution of PL in

membranes is an important factor in the process of division-site selection. At the midcell domain, optimal lipid composition is required for the Z-ring positioning. In *E. coli*, CL-enriched domains were detected at the cell poles and at the division septum, suggesting their involvement in cell division (Kates 1986; Mileykovskaya and Dowhan 2005). Membrane synthesis is also required for cell expansion and might be regulated spatially and temporally in the same manner as cell-wall synthesis. The increased amounts of CL and PE and the incomplete LPS molecules in the mutant strain may, therefore, influence cell-division rate and cell shape by altering the formation of division-site selection and the elongation phase between two divisions. We assume that the incomplete LPS and the altered membrane composition may also be responsible for the lower symbiotic efficiency of MP99 strain. Previous data proved that exopolysaccharide and LPS molecules acting as signals to avoid plant defense reactions may have an important role in plant-bacterium interactions (Stacey et al. 1991).

G3P dehydrogenase encoded by the *glpD* gene has a central function at the crossroad of the glycolytic pathway and the PL biosynthesis pathway. GlpD converts G3P, the key factor in the PL biosynthesis, to di-hydroxy-acetone-phosphate, an intermediate of pyruvate in the glycolytic pathway. Our data suggest that, in *B. japonicum*, the addition of glycerol resulted in a higher expression of the *bat/bto* genes, probably due to the absence of competing GlpR at the overlapping binding site. Further experiments are required to clarify whether the Bat/Bto proteins may also influence directly or indirectly the regulation of *glpD*.

Chromosomally located TA systems of *E. coli* were shown to act as bacterial metabolic stress managers (Buts et al. 2005; Gerdes et al. 2005), associated with the modulation of the global level of translation under various stress conditions and nutrient limitation. In contrast to these data, deletion of the *B. japonicum bat/bto* operon resulted in alterations of several metabolic pathways and defective symbiotic performance, probably due to the changes in LPS and PL composition of the cellular membrane. In conclusion, the *bat/bto* operon seems to be involved in the maintenance of the normal physiological state of the cell, modulating the metabolic rates to a level that may support a better adaptation to environmental conditions.

MATERIALS AND METHODS

Bacterial strains and growth conditions.

Escherichia coli DH5 α (Maniatis et al. 1982) and its derivatives were grown at 37°C in Luria-Bertani (LB) medium (Maniatis et al. 1982) that was supplemented when appropriate with ampicillin (100 μ g/ml), kanamycin (Km) (50 μ g/ml), or tetracycline (Tc) (10 μ g/ml). *Bradyrhizobium japonicum* USDA110 (wild type, spectinomycin-resistant) (Regensburger and Hennecke 1983) was cultivated at 31°C in YEM (yeast-extract-mannitol) (Vincent 1970), PSY (Hahn and Hennecke 1984), or MM (Guerinot et al. 1990) containing the appropriate antibiotics: Sp, 50 μ g/ml; Km, 100 μ g/ml; chloramphenicol, 30 μ g/ml; Tc, 50 μ g/ml; or gentamicin, 150 μ g/ml. When required, a modified MM was used, in which mannitol was replaced by 0.4% (final concentration) of glycerol as the only carbon source present in the medium.

For the determination of generation times, *B. japonicum* wild-type USDA110, MP99, MP119, and MP120 strains were precultured in YEM medium, were washed with 0.9% NaCl solution, and then, were diluted to an OD₆₀₀ of 0.1 in the tested growth media YEM, PSY, and MM. The cultures were grown in flasks in a gyrotory water bath with 200 rpm at 30°C. Samples were taken at the indicated time points, and bacterial

growth was followed by measuring the OD₆₀₀. When required, peptone was added at a final concentration of 0.1%. The experiments were repeated at least six times.

DNA manipulations.

Preparation of plasmid DNA, digestion with restriction enzymes, agarose gel electrophoresis, fragment isolation, cloning procedures, and transformation of *E. coli* cells were performed according to Maniatis and associates (1982). In PCR, *Pfu* polymerase (Fermentas, Vilnius, Lithuania) was used to obtain error-free products.

Construction of strains and plasmids.

Construction of a bat/bto deletion derivative of B. japonicum. For the deletion of the *bat/bto* operon, PCR primers were designed to amplify a 1-kb upstream region and a 1.2-kb downstream region of the operon. The 5' ends of two primers contain a *Bam*HI restriction site each (shown in bold). The sequences of the primers are as follows: BAT1, 5'-CGTGGTTCG TAGAGCTTCTTGA-3' and BAT2, 5'-**GGATCCTGCCAGCA** AGAACCAATA-3' for the amplification of the upstream region; BAT3, 5'-**GGATCCCCCTATCTCAACCGCAC**-3' and BAT4, 5'-GCATCACGGACCGTTTCAA-3' for the amplification of the downstream region. The PCR products were cloned separately in a pBluescript II (SK+) (Alting-Mees and Short 1989) derivative (*Bam*HI site excised from multicloning site) to obtain plasmids pMP73 with the upstream region and pMP74 with the downstream region of the *bat/bto* operon. A *Sma*I-*Bam*HI fragment of pMP74 containing the downstream region was cloned in pMP73, which was digested with the same enzymes. In the resulting plasmid pMP77, the upstream and downstream regions were ligated at the *Bam*HI restriction site. This site was used to introduce a Km-resistance cassette between the two regions, resulting in pMP85. The construct containing the upstream and downstream regions with the Km-resistance cassette was recovered by cutting with *Xho*I-*Spe*I restriction enzymes and was cloned in plasmid pRK290 (Ditta et al. 1980) at the *Eco*RI restriction site, yielding pMP86. This plasmid was conjugally transferred from *Escherichia coli* to *Bradyrhizobium japonicum* wild-type strain by triparental mating using the helper plasmid pRK2013 (Ditta et al. 1980). The *bat/bto* operon was specifically replaced by the Km-resistance cassette as a consequence of the homologous recombination between the upstream and downstream regions present on the chromosome and on pMP86, respectively.

Southern hybridization was performed to confirm the replacement of *bat/bto* genes with the Km-resistance cassette. A 1,351-bp *Hind*III-*Sal*I fragment carrying the Km-resistance cassette was hybridized to the *Bam*HI-digested total DNA of the mutant and wild-type strains to prove the presence of the selectable marker in the mutant. Furthermore, the presence of the resistance cassette and the absence of the *bat/bto* module were also detected by PCR. Primer pairs were designed; in each case, one of the primers was specific for the neighboring genomic region (BAT-UP-F, 5'-ATGGCCGAGGAAGGGATA G-3' and BTO-DW-R, 5'-ACCATGCACCTTCCTGATTT-3' for the upstream and downstream regions, respectively), whereas the other one was specific for the Km cassette (KM-R, 5'-GG CTTCCCAACCTTACCAG-3' and KM-F, 5'-TCGGCATCCA GGAAACCA-3'). Using the corresponding primer pairs (BAT-UP-F and KM-R, KM-F and BTO-DW-R), amplified fragments of correct sizes were detected from the total DNA of the mutant strain, demonstrating that the resistance cassette replaced specifically the *bat/bto* module. Finally, by sequencing of the upstream and downstream regions amplified from the total DNA of the mutant strain by using BAT-1 BAT-2 and

BAT-3 BAT-4, respectively, no further changes were revealed in the neighboring regions at DNA sequence level.

Construction of the complemented strain MP120. In order to confirm that the pleiotropic effects observed in the phenotype of MP99 are all due to the deletion of the *bat/bto* operon, a complemented strain, MP120, was constructed. Primers BAT-PR-F (5'-TCAAACAGACGCATCCCCCGG-3') and BAT-104-R (5'-AGATAGGGCTATGGGTCGTC-3') were used to amplify a fragment consisting of the coding sequence of the *bat/bto* operon and 248 bp upstream of the translation start site of the operon. The amplicon was cloned into the *Eco*RI restriction site of plasmid pRK290 (resulting in the plasmid pMP117) and was introduced into *B. japonicum* MP99 mutant strain by triparental mating, yielding the MP120 complemented strain.

Construction of the revertant strain MP119. To avoid any possible unwanted effect of multiple copies present in the complemented strain, in another experiment, a revertant strain (MP119) was constructed. A DNA fragment containing the *bat/bto* genes and a 1-kb upstream and 1.2-kb downstream region of the operon was amplified by PCR using the primers BAT1 and BAT4. This fragment was cloned in the *Eco*RI restriction site of plasmid pRK290. The resulting plasmid pMP118 was conjugally transferred from *E. coli* to MP99 strain by triparental mating, and the *bat/bto* region was inserted into the chromosome by double homologous recombination. The presence of the wild-type *bat/bto* genes was confirmed by Southern hybridization using as probe a PCR fragment amplified by the BAT1.2 (5'-TCACAACACT GCACCGAC-3') and BAT2.1 (5'-GCCGAATGCAGCGAA ATCC-3') primers. This fragment covers a 677-bp region of the *bat/bto* operon.

Plasmid containing the promoter region of the bat/bto operon. To determine the expression of the *bat/bto* operon, a 379-bp fragment consisting of the 233-bp intergenic region, 144 and 2 bp of the *glpD* and *bat/bto* coding regions, respectively, was amplified with primers BAT1 and BAT2 and was digested with *Bam*HI-*Sal*I restriction enzymes. The promoter-containing fragment was filled by Klenow polymerase and was inserted into plasmid pEP82 (Élö et al. 1998) upstream of the promoterless *lacZ* gene. The resulting plasmid pMP105 was introduced into wild-type, mutant, and complemented *B. japonicum* strains by conjugation.

Plasmids carrying bat, bto, or the bat/bto operon under the IPTG-inducible promoter of pET-28b. To investigate the effect of the ectopic expression of the *bat/bto* module in *E. coli* cells, plasmids containing *bat*, *bto*, or *bat/bto* genes were constructed by cloning the appropriate PCR fragments first in pBluescriptII digested with *Sma*I. The following plasmids were obtained: pMP108 carrying the *bat* gene amplified by the primers B101-F (5'-CTTGCTGCCATGGCCATCA-3') and B102-R (5'-AGC AGGTTACGGCATCT-3'), pMP110 carrying the *bto* gene amplified by the primers B103-F (5'-CGACGAGATGCCATG GACCT-3') and B104-R (5'-AGATAGGGCTATGGGTCGCT-3'), and pMP111 carrying the entire *bat/bto* operon amplified by the primers B101-F and B104-R.

The pBluescriptII derivatives containing the cloned fragments were digested with *Nco*I (present on the fragment) and *Sal*I (present on the multicloning site of the vector), and the inserts were recloned in the *Nco*I-*Sal*I-digested pET-28b vector (Merck, Darmstadt, Germany). The plasmids carrying the *bat* (pMP112), *bto* (pMP113), or *bat/bto* (pMP114) genes under the T7-inducible promoter were transformed in *E. coli* BL21-Gold (DE3) competent cells. Thus, the *Nco*I restriction site of pET-28b and the translational start codon ATG were restored in the plasmids, due to the presence of an *Nco*I site in the sequence of forward primers (underlined).

Viability tests.

E. coli BL21-Gold (DE3) cells with plasmids pMP112, pMP113, pMP114, or the vector pET-28b were grown overnight in LB medium supplemented with Km. The cultures were diluted in the same medium to obtain equal optical densities ($OD_{600} = 0.1$) and were induced with 1 mM IPTG. Cultures were grown at 37°C, and samples were removed to determine OD and viable cell number.

RT-PCR.

RNA was extracted from cells at logarithmic phase using the RNA Easy mini kit from Qiagen (Hilden, Germany). Reverse transcription was performed from identical amounts (1 µg) of RNA obtained from wild-type, MP99, and MP120 strains using the Transcription First Strand cDNA synthesis kit (Roche Applied Science, Indianapolis, IN, U.S.A.). RT-PCR was performed with identical volumes of cDNA samples as templates, using specific primers for the following genes: *hisS* (HIS1, 5'-GAGATGGTCGAGAAGATCC-3' and HIS2, 5'-ATCGTAACGCAAGCTAATC-3'), *pmtA* (PTA1, 5'-CTTCGTCCAGTTCA CCTAT-3' and PTA2, 5'-TTAATCCTTGCGATACACC-3') and *pmtX1* (PTX1, 5'-GGTCTACGATCTCGTGT-3' and PTX2, 5'-AGAGCACCTCGACATTGC-3'). Controls without the reverse transcriptase enzyme or without the template cDNA were also performed. All experiments were repeated three times.

AFM.

Bacteria were grown at 31°C in YEM medium. Aliquots were removed from the cultures at early logarithmic phase and were washed with PBS. To immobilize the cells, muscovite mica surface was coated with a 0.1% (wt/vol) solution of poly-L-lysine (molecular weight >300,000) for at least 2 h. Bacterial adhesion was carried out at room temperature by depositing 20 µl of bacterial suspension onto mica surface, was buffered at pH 7, and was incubated for 20 min. The sample holder containing bacteria was filled with distilled water during experiments.

AFM measurements were carried out with an Asylum MFP-3D head and controller (Asylum Research, Santa Barbara, CA, U.S.A.) in AC mode. The driver program MFP-3D Xop was written in IGOR Pro software (version 5.05b; Wavemetrics, Lake Oswego, OR, U.S.A.). Silicon nitride cantilevers (BioLever Mini BL-AC40TS; Olympus Optical Co., Ltd., Tokyo) with a nominal spring constant of 90 pN/nm were used. Typically 512 × 512-pixel scans were taken at a scan rate of 0.3 to 1.0 lines per second under water. Both trace and retrace images were measured and compared for accuracy, no difference was found between them. A number of at least 40 cells were subjected to the measurements.

To characterize the changes in the mechanical properties of membranes, the elastic (Young's) modulus was determined by force measurements as was described earlier (Balint et al. 2007; Wilhelm et al. 2007), except that force curves were recorded at a constant speed of 600 nm s⁻¹. All experiments were repeated at least four times.

Detection of LPS.

Bacterial cultures of *B. japonicum* wild-type, MP99, and MP120 strains were grown in liquid PSY medium. Cultures (200 µl) of logarithmic phase were pelleted by centrifugation and were washed and extracted with the hot phenol-water method (Kiss et al. 1997). The aqueous phases were pooled and exhaustively dialyzed (membrane cutoff 6,000 to 8,000 kDa) against water. This crude polysaccharide solution was lyophilized and then dissolved in 100 µl of water.

Total polysaccharide extracts were analyzed by sodium deoxycholate-polyacrylamide gel electrophoresis, using 18% poly-

acrylamide gels with deoxycholic acid as detergent (Krauss et al. 1988). Equal amounts of polysaccharide extracts were loaded on gels, except when otherwise described. Sample buffer, gel electrophoresis buffer, and silver staining were used as described by Krauss and associates (1988). Experiments were performed three times.

Lipid extraction.

Cells grown in PSY medium (50 ml) were harvested at $OD_{600} = 0.8$ and were washed twice with PBS, and the wet bacterial cell paste was subjected to lipid extraction procedure according to a modified Bligh and Dyer method (Kates 1986). The final dried lipid extract was immediately dissolved in 300 µl of chloroform/methanol (2:1) and was stored at -20°C.

Fatty-acid analysis of total lipid extracts.

Lipid samples (50 µl) were dried in ampules and trans-methylated with 2 ml of 5% acetyl chloride (in methanol) at 80°C for 2 h. The resulting fatty-acid methyl esters (FAME) were extracted with hexane, the solvent was evaporated, and the residue was dissolved in 50 µl of benzene and was analyzed using the Shimadzu GC-MS-QP2010 (Shimadzu Corporation, Tokyo) equipped with a BPX70 capillary column (10 m × 0.1 mm × 0.2 µm) (SGE Analytical Science Pty Ltd., Ringwood, Australia). A 1-µl aliquot was injected onto the column maintained at 150°C for 2 min and programmed at 6°C per minute from 150 to 215°C and at 20°C per minute to 235°C and then maintained isothermally for 2 min. Fatty-acid composition is given as weight percent (%) of total. The measurements were made in triplicate.

Separation of individual PL.

Individual lipid classes were separated by thin-layer chromatography on Kieselgel 60 silica gel TLC plates (Merck & Co., Inc., Whitehouse Station, NJ, U.S.A.) First, a developing solvent of acetone/petroleum ether (30 to 50°C, 1:3) was used to run to the top of the plate, which was then dried. Second, a chloroform/methanol/acetic acid (65:25:10) solvent was run for 2/3 of the plate. Lipids were visualized by spraying the plate with 0.05% 8-anilinonaphthalene-1-sulfonate in methanol and were identified using authentic standards. Depending on the relative fluorescence, 0.5 to 5 µg of C24:0 fatty acid was applied on the spots as internal standards. The spots were scraped off the plate and transmethylated, and FAME was analyzed as above. All measurements were done in triplicate.

β-galactosidase measurements.

B. japonicum strains grown at 31°C in PSY medium containing the appropriate antibiotics were diluted to $OD_{600} = 0.1$ and were further cultivated to $OD_{600} = 0.5$. The β-galactosidase activity was determined as described previously (Oláh et al. 2001). Glycerol was added to the tested medium when required at a final concentration of 0.04%. Measurements were repeated five times.

Symbiotic interaction with soybean host plant.

Soybean seeds (*Glycine max* var. Pannonia Kincse) were surface-sterilized, were germinated for 3 days at room temperature, and then, were placed in pots containing clay beads (Lodeiro and Favelukes 1999). Aliquots (1 ml) of *B. japonicum* wild-type or MP99 mutant cultures grown in PSY medium were used at the logarithmic growth phase ($OD_{600} = 0.6$; 6.7×10^8 and 7.3×10^8 cells per milliliter, respectively) for inoculation of each plant. For both bacterial strains, 30 soybean plants were analyzed. After 60 days, plants were harvested, and the number of nodules and the dry weight of shoots were determined. To analyze nodule occupancy, 40 nodules were

randomly collected from plants inoculated either by the wild-type or by the MP99 mutant strain and were surface-sterilized by repeated washing with 96% ethanol and, finally, with sterile distilled water. The nodules were crushed and suspended in 0.9% NaCl, and 40 to 80 µl of the solution was placed on YEM agar plates. A total of 200 colonies from each strain type were checked for Km resistance to select for the MP99 mutant strain and for spectinomycin to select for the wild-type strain.

Databases and software.

The complete genomic sequence of *Bradyrhizobium japonicum* was available online at the Kazusa Research Institute RhizoBase website and the BacMap Genome Atlas site. Sequence analyses were done using the ClustalW2 Bioedit program and Promscan.

ACKNOWLEDGMENTS

The authors would like to thank E. Fejes for critical reading of the manuscript. We thank É. Dobó for excellent technical assistance. This work was supported by the Bátyai-Holczer Fund, the Hungarian National Scientific Research Foundation T048706 for G. Váró and 68379 for I. Horváth.

LITERATURE CITED

Alting-Mees, M. A., and Short, J. M. 1989. pBluescript II: Gene mapping vectors. *Nucleic Acids Res.* 17:9494.

Amitai, S., Yassin, Y., and Engelberg-Kulka, H. 2004. *MazF*-mediated cell death in *Escherichia coli*: A point of no return. *J. Bacteriol.* 186:8295-8300.

Arcus, V. L., Backbro, K., Roos, A., Daniel, E. L., and Baker, E. N. 2004. Distant structural homology leads to the functional characterization of an archaeal PIN domain as an exonuclease. *J. Biol. Chem.* 279:16471-16478.

Bálint, Z., Krizbai, I. A., Wilhelm, I., Farkas, A. E., Pardutz, A., Szegletes, Z., and Varo, G. 2007. Changes induced by hyperosmotic mannitol in cerebral endothelial cells: An atomic force microscopic study. *Eur. Biophys. J.* 36:113-120.

Bodogai, M., Ferenczi, S., Bashtovyy, D., Miclea, P., Papp, P., and Dusha, I. 2006. The *ntfPR* operon of *Sinorhizobium meliloti* is organized and functions as a toxin-antitoxin module. *Mol. Plant-Microbe Interact.* 19:811-822.

Boncompagni, E., Osteras, M., Poggi, M. C., and Le Rudulier, D. 1999. Occurrence of choline and glycine betaine uptake and metabolism in the family *Rhizobiaceae* and their roles in osmoprotection. *Appl. Environ. Microbiol.* 65:2072-2077.

Broun, A., Liu, S., and Lewis, K. 2000. A dose-response study of antibiotic resistance in *Pseudomonas aeruginosa* biofilms. *Antimicrob. Agents Chemother.* 44:640-646.

Bunker, R. D., McKenzie, J. L., Baker, E. N., and Arcus, V. L. 2008. Crystal structure of PAE0151 from *Pyrobaculum aerophilum*, a PIN-domain (VapC) protein from a toxin-antitoxin operon. *Proteins* 72:510-518.

Buts, L., Lah, J., Dao-Thi, M. H., Wyns, L., and Loris, R. 2005. Toxin-antitoxin modules as bacterial metabolic stress managers. *Trends Biochem. Sci.* 30:672-679.

Carrion, M., Bhat, U. R., Rheus, B., and Carlson, R. W. 1990. Isolation and characterization of the lipopolysaccharides from *Bradyrhizobium japonicum*. *J. Bacteriol.* 172:1725-1731.

Christensen, S. K., Mikkelsen, M., Pedersen, K., and Gerdes, K. 2001. RelE, a global inhibitor of translation, is activated during nutritional stress. *Proc. Natl. Acad. Sci. U.S.A.* 98:14328-14333.

Danilova, L. V., Gelfand, M. S., Lyubetsky, V. A., and Laikova, O. N. 2003. Computer-assisted analysis of regulation of the glycerol-3-phosphate metabolism in genomes of Proteobacteria. *Mol. Biol.* 37:716-722.

Dénarié, J., Debelle, F., and Promé, J.-C. 1996. *Rhizobium* lipochitoooligosaccharide nodulation factors: Signaling molecules mediating recognition and morphogenesis. *Annu. Rev. Biochem.* 65:503-535.

Ditta, G., Stanfield, S., Corbin, D., and Helinski, D. R. 1980. Broad host range DNA cloning system for gram-negative bacteria: Construction of a gene bank of *Rhizobium meliloti*. *Proc. Natl. Acad. Sci. U.S.A.* 77:7347-7351.

Donegan, N. P., and Cheung, A. L. 2009. Regulation of the *mazEF* toxin-antitoxin module in *Staphylococcus aureus* and its impact on *sigB* expression. *J. Bacteriol.* 191:2795-2805.

Élö, P., Semsey, S., Kereszt, A., Nagy, T., Papp, P., and Orosz, L. 1998. Integrative promoter cloning plasmid vectors for *Rhizobium meliloti*. *FEMS (Fed. Eur. Microbiol. Soc.) Microbiol. Lett.* 159:7-13.

Gerdes, K. 2000. Toxin-antitoxin molecules may regulate synthesis of macromolecules during nutritional stress. *J. Bacteriol.* 182:561-572.

Gerdes, K., Christensen, S. K., and Lobner-Olesen, A. 2005. Prokaryotic toxin-antitoxin stress response loci. *Nat. Rev. Microbiol.* 3:371-382.

Gibson, K. E., Kobayashi, H., and Walker, G. C. 2008. Molecular determinants of a symbiotic chronic infection. *Annu. Rev. Genet.* 42:413-41.

Guerinot, M. L., Meidl, E. J., and Plessner, O. 1990. Citrate as a siderophore in *Bradyrhizobium japonicum*. *J. Bacteriol.* 172:3298-3303.

Hacker, S., Sohlenkamp, C., Aktas, M., Geiger, O., and Narberhaus, F. 2008. Multiple phospholipid *N*-methyltransferases with distinct substrate specificities are encoded in *Bradyrhizobium japonicum*. *J. Bacteriol.* 190:571-580.

Hahn, M., and Hennecke, H. 1984. Localized mutagenesis in *Rhizobium japonicum*. *Mol. Gen. Genet.* 193:46-52.

Hayes, F. 2003. Toxins-antitoxins: Plasmid maintenance, programmed cell death and cell cycle arrest. *Science.* 301:1496-1499.

Hazan, R., Sat, B., and Engelberg-Kulka, H. 2004. *Escherichia coli mazEF*-mediated cell death is triggered by various stressful conditions. *J. Bacteriol.* 186:3663-3669.

Horváth, I., Mansourian, A. R., Vigh, L., Thomas, P. G., Joó, F., and Quinn, P. J. 1986. Homogeneous catalytic hydrogenation of the polar lipids of pea chloroplasts in situ and the effects on lipid polymorphism. *Chem. Phys. Lipids* 39:251-264.

Jensen, R. B., and Gerdes, K. 1995. Programmed cell death in bacteria: Proteic plasmid stabilization systems. *Mol. Microbiol.* 17:205-210.

Jones, K. M., Kobayashi, H., Davies, B. W., Taga, M. E., and Walker, G. C. 2007. How rhizobial symbionts invade plants: The *Sinorhizobium-Medicago* model. *Nat. Rev.* 5:619-633.

Jørgensen, M. G., Pandey, D. P., Jaskolska, M., and Gerdes, K. 2009. HicA of *Escherichia coli* defines a novel family of translation-independent mRNA interferases in bacteria and archaea. *J. Bacteriol.* 191:1191-1199.

Kates, M. 1986. Techniques in lipidology. Pages 232-254 in: Isolation and Identification of Lipids, 2nd ed. R. H. Burdon, P. H. van Knippenberg, eds. Elsevier, Amsterdam.

Keren, I., Shah, D., Spoering, A., Kaldalu, N., and Lewis, K. 2004. Specialized persister cells and the mechanism of multidrug tolerance in *Escherichia coli*. *J. Bacteriol.* 186:8172-8180.

Kiss E, Reuhs, B. L., Kim, J. S., Kereszt, A., Petrovics, G., Putnok, P., Dusha, I., Carlson, R. W., and Kondorosi, A. 1997. The *rpkGHI* and *-J* genes are involved in capsular polysaccharide production by *Rhizobium meliloti*. *J. Bacteriol.* 179:2132-2140.

Korch, S. B., Contreras, H., and Clark-Curtiss, J. E. 2009. Three *Mycobacterium tuberculosis* Rel toxin-antitoxin modules inhibit mycobacterial growth and are expressed in infected human macrophages. *J. Bacteriol.* 191:1618-1630.

Krauss, J. H., Weckesser, J., and Mayer, H. 1988. Electrophoretic analysis of lipopolysaccharides of purple nonsulfur bacteria. *Int. J. Syst. Bacteriol.* 38:157-163.

Lehnher, H., Magnuson, R., Jafri, S., and Yarmolinsky, M. B. 1993. Plasmid addiction genes of bacteriophage P1: *doc*, which causes cell death on curing of prophage, and *phd*, which prevents host death when prophage is retained. *J. Mol. Biol.* 233:414-428.

Lodeiro, A. R., and Favelukes, G. 1999. Early interactions of *Bradyrhizobium japonicum* and soybean roots: Specificity in the process of adsorption. *Soil Biol. Biochem.* 31:1405-1411.

Lewis, K. 2005. Persister cells and the riddle of biofilm survival. *Biochemistry-Moscow* 70:267-274.

Magnuson, R., and Yarmolinsky, M. B. 1998. Corepression of the P1 addiction operon by Phd and Doc. *J. Bacteriol.* 180:6342-6351.

Makarova, K. S., Aravind, L., Galperin, M. Y., Grishin, N. V., Tatusov, R. L., Wolf, Y. I., and Koonin, E. V. 1999. Comparative genomics of the Archaea (Euryarchaeota): Evolution of conserved protein families, the stable core, and the variable shell. *Genome Res.* 9:608-628.

Maniatis, T., Fritsch, E. F., and Sambrook, J. E. 1982. *Molecular Cloning. A laboratory Manual.* Cold Spring Harbor Laboratory, Cold Spring Harbor, NY, U.S.A.

Marianovsky, I., Aizenman, E., Engelberg-Kulka, H., and Glaser, G. 2001. The regulation of the *Escherichia coli mazEF* promoter involves an unusual alternating palindrome. *J. Biol. Chem.* 276:5975-5984.

Martínez-Morales, F., Schobert, M., López-Lara I. M., and Geiger O. 2003. Pathways for phosphatidylcholine biosynthesis in bacteria. *Microbiology* 149:3461-3471.

Mattison, K., Wilbur, J. C., So, M., and Brennan, R. G. 2006. Structure of FitAB from *Neisseria gonorrhoeae* bound to DNA reveals a tetramer of toxin-antitoxin heterodimers containing PIN domains and ribbon-helix-helix motifs. *J. Biol. Chem.* 281:37942-37951.

- Mileykovskaya, E., and Dowhan, W. 2005. Role of membrane lipids in bacterial division-site selection. *Curr. Opin. Microbiol.* 8:135-142.
- Mine, N., Guglielmini, J., Wilbaux, M., and Van Melderen, M. 2009. The decay of the chromosomally encoded *ccd*_{O157} toxin-antitoxin system in the *Escherichia coli* species. *Genetics*, 181:1557-1566.
- Oláh, B., Kiss, E., Györgypál, Z., Borzi, J., Cinege, G., Csanádi, G., Batut, J., Kondorosi, A., and Dusha, I. 2001. Mutation in the *nttR* gene, a member of the *vap* gene family, increases the symbiotic efficiency of *Sinorhizobium meliloti*. *Mol. Plant-Microbe Interact.* 14:887-894.
- Pandey, D. P., and Gerdes, K. 2005. Toxin-antitoxin loci are highly abundant in free-living but lost from host-associated prokaryotes. *Nucleic Acids Res.* 33:966-976.
- Pedersen, K., Christensen, S. K., and Gerdes, K. 2002. Rapid induction and reversal of a bacteriostatic condition by controlled expression of toxins and antitoxins. *Mol. Microbiol.* 45:501-510.
- Pedersen, K., Zavialov, A. V., Pavlov, M. Y., Elf, J., Gerdes, K., and Ehrenberg, M. 2003. The bacterial toxin RelE displays codon-specific cleavage of mRNAs in the ribosomal A site. *Cell*. 112:131-140.
- Puskás, L. G., Nagy, Z. B., Kelemen, J. Z., Rübberg, S., Bodogai, M., Becker, A., and Dusha, I. 2004. Wide-range transcriptional modulating effect of *nttR* under microaerobiosis in *Sinorhizobium meliloti*. *Mol. Gen. Genomics* 272:275-289.
- Regensburger, B., and Hennecke, H. 1983. RNA polymerase from *Rhizobium japonicum*. *Arch. Microbiol.* 135:103-109.
- Rietveld, A. G., Killian, J. A., Dowhan, W., and de Kruijff, B. 1993. Polymorphic regulation of membrane phospholipid composition in *Escherichia coli*. *J. Biol. Chem.* 15:12427-33.
- Sat, B., Hazan, R., Fisher, T., Khaner, H., Glaser, G., and Engelberg-Kulka, H. 2001. Programmed cell death in *Escherichia coli*: Some antibiotics can trigger *mazEF* lethality. *J. Bacteriol.* 183:2041-2045.
- Smith, J. A., and Magnuson, R. D. 2004. Modular organization of the Phd repressor/antitoxin protein. *J. Bacteriol.* 186:2692-2698.
- Stacey, G., So, J. S., Roth, L. E., Lakshmi, S. K. B., and Carlson, R. W. 1991. A lipopolysaccharide mutant of *Bradyrhizobium japonicum* that uncouples plant from bacterial differentiation. *Mol. Plant-Microbe Interact.* 4:332-340.
- Tsilibaris, V., Maenhaut-Michel, G., Mine, N., and Van Melderen, L. 2007. What is the benefit of *Escherichia coli* of having multiple toxin-antitoxin systems in its genome? *J. Bacteriol.* 189:6101-6108.
- Vigh, L., Escribá, P. V., Sonnleitner, A., Sonnleitner, M., Piotto, S., Maresca, B., Horváth I., and John L. Harwood. 2005. The significance of lipid composition for membrane activity: New concepts and ways of assessing function. *Progr. Lipid. Res.* 44:303-344.
- Vincent, J. M. 1970. A manual for the practical study of root nodule bacteria. International Biological Program Handbook 15. Blackwell Scientific Publications, Oxford.
- Wilhelm, I., Farkas, A. E., Nagyösi, P., Váró, G., Bálint, Z., Végh, G. A., Couraud, P.-O., Romero, I. A., Weksler, B., and Krizbai, I. A. 2007. Regulation of cerebral endothelial cell morphology by extracellular calcium. *Phys. Med. Biol.* 52:6261-6274.
- Yang, B., and Larson, T. J. 1996. Action at a distance for negative control of transcription of the *glpD* gene encoding *sn*-glycerol 3-phosphate dehydrogenase of *Escherichia coli* K-12. *J. Bacteriol.* 178:7090-7098.
- Yang, B., and Larson, T. J. 1998. Multiple promoters are responsible for transcription of the *glpEGR* operon of *Escherichia coli* K-12. *Biochim. Biophys. Acta* 1396:114-126.
- Ye, S. Z., and Larson, T. J. 1988. Structures of the promoter and operator of the *glpD* gene encoding aerobic *sn*-glycerol-3-phosphate dehydrogenase of *Escherichia coli* K-12. *J. Bacteriol.* 170:4209-4215.
- Zhang, Y., Zhang, J., Hoeflich, K. P., Ikura, M., Qing, G., and Inouye, M. 2003. MazF cleaves cellular mRNAs specifically at ACA to block protein synthesis in *Escherichia coli*. *Mol. Cell* 12:913-923.

AUTHOR-RECOMMENDED INTERNET RESOURCES

- BacMap Genome Atlas: wishart.biology.ualberta.ca/BacMap
- European Molecular Biology Laboratory-European Bioinformatics Institute ClustalW2 website: www.ebi.ac.uk/Tools/clustalw2/index.html
- Kazusa Research Institute RhizoBase webpage: bacteria.kazusa.or.jp/rhizobase
- Queen's University's Promscan: molbiol-tools.ca/promscan